The Measurement and Interpretation of Actively Modulated Static Ankle Impedance using a Theraputic Robot

by

Patrick Ho

Submitted to the Department of Mechanical Engineering
in partial fulfillment of the requirements for the degree of

Master of Science in Mechanical Engineering

at the

MASSACHUSETTS INSTITUTE OF TECHNOLOGY

June 2010

Author .....
Department of Mechanical Engineering
May 18, 2010

Certified by .....
Neville Hogan
Professor
Thesis Supervisor

Accepted by .....
David E. Hardt
Chairman, Department Committee on Graduate Theses

The Measurement and Interpretation of Actively Modulated Static Ankle Impedance using a Theraputic Robot

by

Patrick Ho

Submitted to the Department of Mechanical Engineering
on May 18, 2010, in partial fulfillment of the
requirements for the degree of
Master of Science in Mechanical Engineering

Abstract

In this thesis, I conducted an in-vivo study providing measurementsof human static ankle mechanical impedance. Accurate measurements of ankle impedance when muscles were voluntarily activated were obtained using a therapeutic robot, Anklebot, and an electromyographic recording system. Important features of ankle impedance, and their variation with muscle activity, are discussed, including magnitude, symmetry and directions of minimum and maximum impedance. Voluntary muscle activation has a significant impact on ankle impedance, increasing it by up to a factor of three in our experiments. Furthermore, significant asymmetries and deviations from a linear two-spring model are present in many subjects, indicating that ankle impedance has a complex and individually idiosyncratic structure. I propose the use of Fourier series as a general representation, providing both insight and a precise quantitative characterization of human static ankle impedance.

Thesis Supervisor: Neville Hogan
Title: Professor

Acknowledgments

First, I would like to give thanks to my advisor, Neville Hogan, for his guidance and his patience throughout.

Special thanks go out to all my labmates, especially Hyunglae Lee and Mohammed Rastgaar.

This research was generously supported by a grant from Toyota Motor Corporation's Partner Robot division, and many thanks go to them for their strong interest in the project.

Last, but not least, I want to thank my family for all the love and support they've given me throughout this process. Thanks Mom, Dad, Jessica, and Randy for being my first line of defense against what life has to throw at me.

Contents

List of Figures

List of Tables

Chapter 1

Introduction and Literature on Mechanical Impedance

Physical and occupational therapists employ motion therapy for a wide variety of physical ailments. The condition of the ankle (or other joints) is often characterized using a subjective scale of muscle tone called the Modified Ashworth Scale [5]. Physical condition can often be related to ankle impedance, with neurological conditions leading to abnormally high stiffnesses after strokes (ibid). The Modified Ashworth Scale calls upon the therapist to evaluate the increase in muscle tone in terms of slight, minimal, marked, considerable, and rigid. The development of a new widely applicable, but quantitative, scale of ankle impedance could provide more clarity for the therapist than those five categories, especially if it is well tailored to the specific biomechanics of the ankle.

This thesis describes an effort to analyze the features of the human ankle's mechanical impedance (the relationship between the rotational motion of the foot relative to the shank and the torque exerted about the ankle joint) in a standardized and quantitative fashion using data collected from a therapeutic robot. With the advent of quantitative descriptions of ankle impedance, more understanding and insight into human physiology may emerge, describing not only the magnitude of ankle impedance, but also symmetry properties and directions of minimum and maximum impedance. Unlike a simple spring, ankle impedance

is actively modulated: when subjects produce one way torque or cocontraction with their leg muscles, we expect to see impedance change relative to passive conditions. With a system capable of measuring ankle impedance under both passive and active conditions, the number of potentially useful therapeutic measurements increases dramatically.

Sophisticated tools for measuring ankle impedance may improve clinical treatments and produce data useful for designing human-robot interaction. With objective and precise quantitative measurement, databases containing individual treatment histories as well as data on the general population can be established. The effects of various physical ailments and treatments can be compared among subjects, potentially improving clinical practice. Human-robot interaction may also benefit from a better quantification of human ankle impedance, enabling mobility assist devices and external robots to better predict and model the consequences of interacting physically with the human about the ankle joint.

Prior work has provided detailed quantitative assessment of multi-variable mechanical impedance about other joints in the human body. The shoulder and elbow joints have been broadly studied, notably by Mussa-Ivaldi et al [2], and more recently by Gomi and Osu [1]. Upper-limb impedance is configuration dependent, with stiffness ellipses varying depending on joint angle. However, it is unclear whether a stiffness ellipse provides a sufficiently general description of multi-variable static impedance, either in the upper limb or in other joints such as the wrist or ankle.

Significant efforts have been made to quantitatively measure ankle impedance, but the majority of studies have focused on the impedance along a single degree of freedom (DOF). Selles et al. and Yeh et al. measured passive ankle impedance in dorsiflexion and plantarflexion in stroke patients [6]. Sinkjaer et al. evaluated ankle impedance in healthy subjects as a function of muscle activity in the dorsiflexion-plantarflexion directions [7]. Zinder et al. evaluated dynamic ankle impedance in the inversion-eversion directions [9]. Here we report measurements of static ankle impedance in combined degrees of freedom, and from the data suggest the use of Fourier series fitting as a fully general interpretive tool to assist the further quantification of ankle impedance. We also report the significant dependence of ankle static

impedance on the voluntary modulation of muscle activation, indicating humans maintain significant control over the impedance of their ankle.

Anklebot, a highly back-drivable therapeutic robot, was used to carry out our measurements in a two dimensional angular space, applying ramp perturbations to the foot and inducing a resulting torque on the foot. It is designed to provide up to 17 Nm of torque and to work with sitting, standing, or walking humans [4]. The foot is free to rotate relative to the shank along three degrees of freedom. By extending or retracting the actuators in a linked fashion, Anklebot can alter the position of the foot in dorsiflexion and plantarflexion. By moving the actuators in opposite directions, Anklebot alters the position of the foot in inversion-eversion.

Though Anklebot is a powerful therapeutic and research tool, significant modifications had to be made in order to make it suitable for the study described here. New procedures had to be developed for the use of the robot, and new software had to be created integrating the Anklebot with an electromyographic system. All of that work is detailed in the following chapters. Chapter 2 details coding modifications made in the course of thesis work. Chapter 3 details the rationale behind the experimental method (Appendix A details the step-by-step method itself). Chapter 4 reports the data collected from human subjects with Anklebot. Chapter 5 discusses new analysis methods for ankle impedance, and Chapter 6 recommends future work based on the work contained herein.

Chapter 2

Code Modifications

2.1 The Structure of Anklebot Code

Anklebot runs on a proprietary robot kernel module designed by InMotion Technology of Cambridge, MA. The IMT kernel, running in Linux environment, drives the many hardware components used in Anklebot operation. The particular system on which the experiments described here were run used a Real-Time Linux operating system. Real-Time Linux allows a small amount of code to be run at a fixed frequency, while running other code as computer resources allow. The file system of the IMT software deserves special mention. The kernel is saved in a crob folder, short for C Robot. Files belonging to the kernel are written in the C programming language, while files accessible to the robots user are written in the tcl/Tk programming language. The kernel is responsible for communicating with sensors, actuators, and junction box input, and the user programs are responsible for communicating with the machine operators. In the RTLinux environment, the robot kernel must be compiled and loaded before the robot will function. The kernel is recompiled by using the make command (built into the crob folder) after any changes are made to it. Once the kernel is loaded, special user programs are able to access system variables and command the robot. Figure 2.1 shows the two layer architecture of the anklebot software. User software interacts with the kernel through a feature called shared memory (shm), where variables can be read and written by

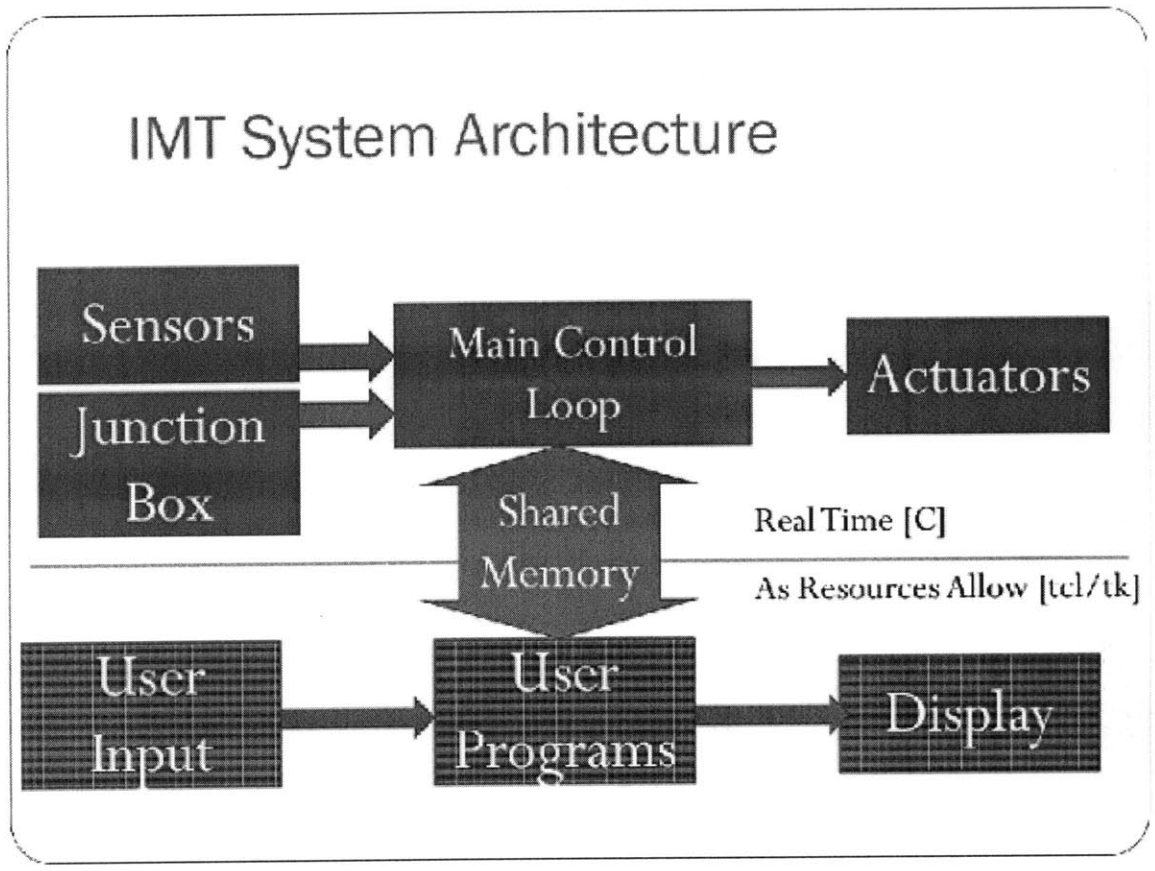

Figure 2-1: IMT Robot Software Architecture

both kernel programs and user level programs. Paralleling the software architecture, there is a shm.c and a shm.tcl file detailing memory access protocols for both types of software. These two files interact through a special reference file called cmdlist.tcl, which functions as a master index where physical memory addresses are assigned to both c and tcl variables. The file cmdlist.tcl is an extremely useful guide and comprehensive to system variables for the programmer.

The primary C program in crob is main.c, which contains the main data structures (structs) and the main control loop of the robot. The robot is constructed around three major objects, Rob, Ob, and Daq. Rob contains all the variables pertaining to the actual

robot, such as actuator state and commanded voltages. Ob contains all variables pertaining to the environment and system operation, the vast majority of system variables fall into ob by default. Daq contains variables pertaining to data input and output, including the ports of the Data Acquisition Card (DAQ). These data structures are used to provide some measure of organization to the myriad variables used in robot operations.

Main.c runs a loop updating all system values every tick. This loop first reads sensors and records their values. The loop then computes control parameters. Next it writes output to actuators, and for the remainder of the time it allows less critical functions to operate. The main.c file does not actually contain any controllers, logging functions, or sensor reading functions. Instead, main.c calls upon separate files that detail those functions, and these functions can be modified by programmers and researchers without directly affecting the function of the main loop.

2.2 Goals for Modifications

Several new programs were developed with the goals of automating collection of ankle impedance data and providing experimental controls. User programs for automating data collection were written in accordance to the experimental protocol laid out in Chapter 3. The programs written for experimental controls provide visual feedback for EMG self-regulation. The challenge of designing a visual system for EMG display requires that the programmer deal with the challenge of real time EMG amplitude estimation of a priori unknown EMG amplitudes. EMG signals are by nature very noisy and variable, sensitive to ambient electromagnetic interference, motion of the electrodes on the skin, and the conductivity of the skin. The variability of the EMG signal was reduced by using a moving-average amplitude estimator, spreading the amplitude estimate over two hundred milliseconds in our particular implementation. The new programs also allowed the user to scale the visual display to a level appropriate to the average EMG activity level.

Four new user programs were created in the course of the project:

2.2.1 CocontractionStudy.tcl

This program is used to run the 24 direction protocol for passive, active, and cocontraction experiments. The program outputs ramp and hold motion patterns to Anklebot using *movebox*, the built in point-to-point move function. It accepts user-defined magnitude, speed, and pause times and then computes the appropriate ramp input in IE and DP degrees of freedom. CocontractionStudy.tcl was also modified to begin the EMG amplitude estimation controller.

2.2.2 Wedgedisp.tcl

This program is used to visually display robot variables. It built upon display.tcl, a program used to display numbers stored in shared memory (shm). By adding an extra graphics box, using tools from the Tk add-on to the Tcl programming language, the utility of display for subject use was increased dramatically. The new graphics box draws an indicator bar that scales in proportion to the absolute value of the variable, providing both size and position cues to the user. This program refreshes via shm, providing a real time display of six variables simulatenously. The size of the bars can be rescaled in the code of wedgedisplay.tcl by changing the arr(x,ref) variable (where x is 0-5).

2.2.3 Acenter_emg.tcl

This program is used for the stochastic impedance estimation function. It was written to add on EMG amplitude estimation to the existing acenter_emg.tcl file. It functions similarly to acenter.tcl, creating a point controller that attempts to bring the foot to the centered position.

2.2.4 converter

This file converts the data output of CocontractionStudy.tcl into a usable ascii format

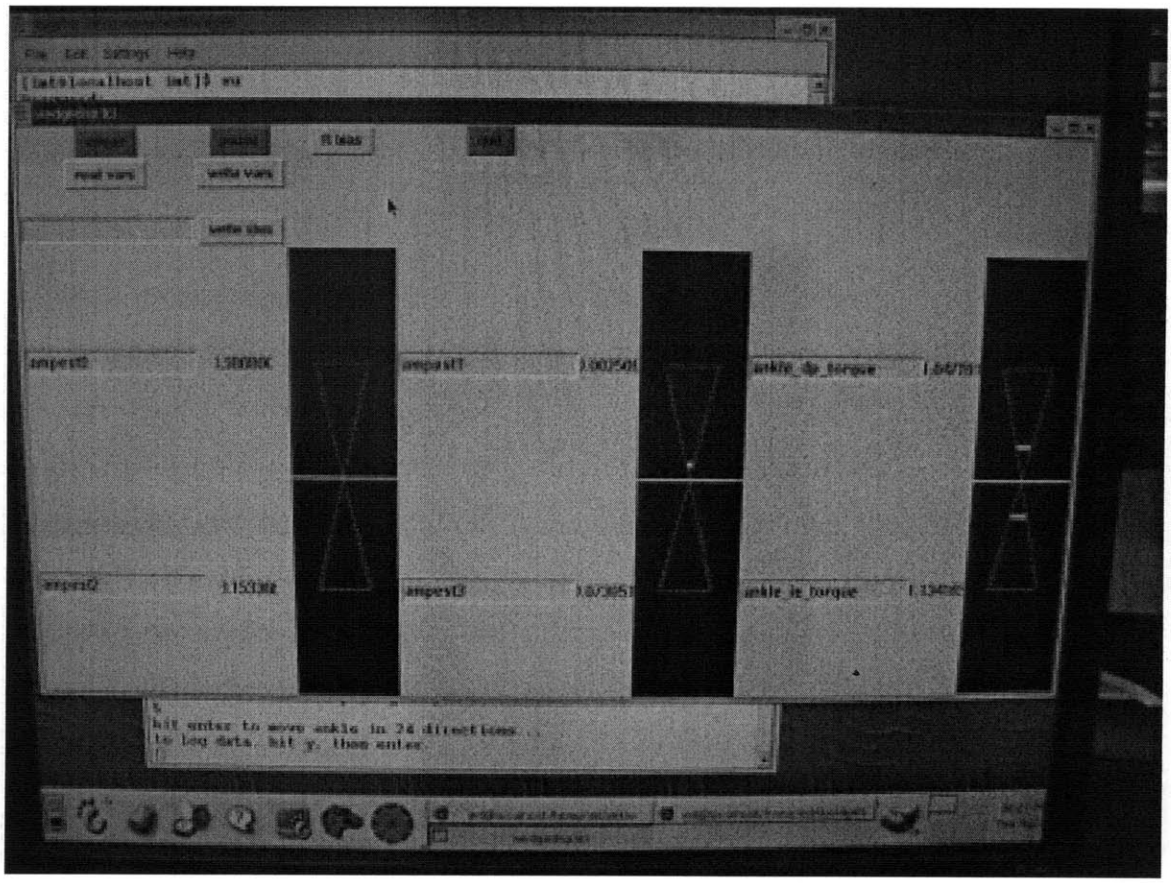

Figure 2-2: Screenshot of visual feedback program wedgedisp.tcl

2.3 Kernel Modifications

Most modifications to the anklebot kernel were made within a few locations. The primary addition to the kernel was an EMG amplitude estimator object and the code necessary to operate this estimator. This object reads in the absolute value of the most recent DAQ value from a particular channel. It then writes this value to an array of previous DAQ input values (writing over the oldest value), and computes the average value along the entire array. Thus the amplitude estimator creates a moving average estimate of the input amplitude accessible in real time with minimal computation.

2.3.1 robdecls.h

robdecls.h is the C header file where variables and data structures relevant to system operation are declared. Two data structures were modified. A new struct declaration for emg_buffer_s was created, detailing the variables necessary to estimate a moving average from a DAQ channel. Eight instances of emg_buffer_s were added to the existing struct ob_s, enabling the kernel to estimate the magnitude of eight input channels.

2.3.2 an_sensact.c

Many system variables are initialized within the function $void\ ankle\_init(void)$. An initialization for all eight estimate channels was added, and a function $void\ initbuff(EMG\_buffer*\ channel, double*\ trgt, double*\ array1)$ was written to perform this initialization.

2.3.3 cmdlist.tcl

Three new groups of variables were made accessible to shared memory. The variable ampest represents the output of a particular EMG amplitude estimate channel (ampest0 estimates the first DAQ channel, ampest1 estimates the second, and so on). The variable displayref allows the user to capture the output of a particular box within the wedgedisp.tcl display program (by writing 1 to displayref0, the program will output the current value of the first

variable being displayed in the display program). The variable cmd_est_buff allows user programs to start, stop, and reset amplitude estimators.

2.3.4 an_ulog.c

Two logger functions were added to the kernel. This logger function writes select variables at each clock tick to a logging file. The new logging functions were made to support both the static and dynamic impedance estimates. The function $void\ write\_ankle\_fifo\_emg\_fn(void)$ logs the variables for the static impedance estimate, and the function $void\ write\_ankle\_fifo\_raw\_signals\_fn(void)$ logs the variables for the dynamic impedance estimate.

2.3.5 an_uslot.c

The bulk of changes to the anklebot code were made in the ankle controller function. A pair of novel controller functions, $void\ ankle\_point\_ctl\_emg(u32)$ and $void\ ankle\_ctl\_emg(u32)$, were written for amplitude estimation. These functions consist of existing ankle controllers, with new code that updates the EMG buffer each time the controller is called. If the value of buffer state variable $ob- > buff\_commands[k]$ is 1, the controller will begin EMG buffer operation. If the value of $ob- > buff\_commands[k]$ is 2, the controller will remove the DC bias from the channel estimates. If the value of $ob- > buff\_commands[k]$ is 10 the controller will stop EMG buffer operation. The actual EMG amplitude estimator is updated in $void\ updateemgbuff(EMG\_buffer * channel)$. This function has two modes, the regular amplitude estimation mode and a DC bias removal mode. In both cases the primary job of this function is to add the latest input from the DAQ card to a list of the most recent values and remove old input. $Updateemgbuff(EMG\_buffer * channel)$ then either updates the estimate of the EMG amplitude or the estimate of the bias. Three other functions were made, to correctly initialize variables when starting the buffer, stopping the EMG buffers, and estimating the bias [$void\ stop\_emgbuff(EMG\_buffer * channel)$, $void\ set\_emgbuff\_bias(EMG\_buffer * channel)$, $void\ start\_emgbuff(EMG\_buffer * channel)$].

2.3.6 pl_uslot.c

This file contains the master list of controller functions in the function *void init_slot_fns(void)* . The new controllers added to the list were *void ankle_point_ctl_emg(u32)* and *void ankle_ctl_emg(u32)* described in the previous section.

2.3.7 pl_ulog.c

This file contains the master list of logging functions in the function *void init_log_fns(void)*. The two logger functions written in an_ulog.c were added to the list, *void write_ankle_fifo _emg_fn(void)* and *void write_ankle_fifo_raw_signals_fn(void)*.

Chapter 3

Experimental Methodology for Measuring Ankle Impedance

3.1 Measurement Process

The goal of our experiment was to elucidate the change in human ankle impedance as muscle activation is varied. The relation of the displacement history to the torque history of the foot represents the impedance of the ankle. In the studies described here, we estimated the steady-state relationship of torque as a function of displacement, also known as the static impedance. Dynamic relations from displacement to torque are also possible, with higher derivatives of displacement affecting measured torque at a particular instant in time, but the methods of this section are not appropriate for measuring dynamic impedance. Human muscles exhibit characteristic activation-dependent force-length characteristics, and therefore we expected that in accordance with the force length curves described in Zajac (1989) [8], ankle impedance may increase with the activation of muscle and would especially increase in cocontraction. A detailed step by step experimental method is described in Appendix A, here the motivations behind the measurement process are described.

At its most basic, measuring impedance is analogous to stretching a spring and measuring the resulting force. With more complicated systems, there may be rate dependent

impedances due to either basic physical processes or system feedback. A well designed perturbation is necessary in order to control for the contributions of different system components to impedance. For example, involuntary muscle reflexes may change ankle impedance if the velocity or magnitude of the perturbation is large. We selected a slow ramp profile in order to measure as accurately as possible the static ankle impedance. On face, a true static measurement would seem to be no more than a measure of impedance as the ankle is held in place after being perturbed from an initial position. However, this ramp-and-hold procedure must deal with the interpretation of the evolution of steady-state ankle impedance (which is not necessarily constant, assuming torque begins to diminish or increase as the ankle is held). We avoid this problem by ensuring the ankle is not held in place and measuring the torque-position relationship as the position is slowly changed, eliminating as much as possible time dependent changes in ankle impedance.

Anklebot was programmed to apply terminated ramp perturbations to the human ankle joint in the frontal and sagittal planes. Under our convention, zero degrees of perturbation corresponded to pure eversion; 15 degrees meant that the foot was placed $\cos(15^o)$ in eversion for every $\sin(15^o)$ it was placed in dorsiflexion; 90 degrees corresponded to pure dorsiflexion, and so on. To minimize the likelihood of evoking spindle-mediated stretch reflexes, the ramp velocity was set at 5 degrees per second, and ramps terminated at 20 degrees from the center position. In order to adequately sample the measurement space, the ankle was perturbed in 24 directions (beginning at 0^o, incrementing by 15^o, and finishing with 345^o) A total of 48 movements, one increasing and one decreasing ramp per direction, were made per measurement. The foot was held briefly at the minimum or maximum of the ramp, for a period of 100ms. The foot was initially centered at 90 degrees relative to the lower limb with no inversion or eversion. A proportional-plus-derivative (PD) position controller with gains (Kp = 100 Nm/rad, Kd = 2 Nm-s/rad) was used to move the ankle along the commanded trajectory. The position and torque histories imposed by this PD controller were recorded at 200Hz.

The studies reported here recruited young unimpaired subjects who had no reported his-

tory of neuromuscular disorders involving the ankle. However, the methods used are general and can be used with subjects of any age. Subjects gave informed consent to participate in the study following procedures approved by MITs institutional review board. Accordingly, subjects were introduced to the equipment, told the requirements of the experiment, and were were informed that they would wear Anklebot. They were also informed that they would be connected to electromyographic equipment (EMG) and be subject to torques and movements applied to their leg.

Static ankle impedance was measured under various experimental conditions of voluntary muscle activation. In the active study, subjects were asked to activate a single muscle at a constant EMG signal level. Activation of two muscles was studied: tibialis anterior (a dorsiflexor) and soleus (a plantarflexor). They were provided with visual feedback in order to minimize variability of the EMG signal. In the cocontraction study, subjects were asked to activate several muscles at the same time, and to maintain the tibialis anterior and soleus at high activity levels (as indicated by EMG) while limiting their variability. The target EMG level for each subject was calibrated experimentally by finding the EMG amplitude corresponding to a sufficiently large target torque level for that muscle, at least 3.2 N-m in the direction of the muscles primary action.

3.2 Self Regulation of EMG

Since torque was generated and measured using the robot, an alternate measure of the subjects voluntary torque generation was required. Surface electromyograms (EMG) were recorded to determine muscle activity level. Electrodes were attached to the skin over the major superficial leg muscles: tibialis anterior, peroneus longus, soleus, and gastrocnemius (Figure 3.1). The EMG recordings provided a check on subjects adherence to experimental instructions. In the passive condition subjects were asked to relax and not interfere with the robots motions. On the EMG, this appears as if none of the electrodes are recording signals of significant amplitude. For each active condition, subjects were asked to activate either the tibialis anterior muscle or the soleus muscle tonically. The active condition ideally appears as

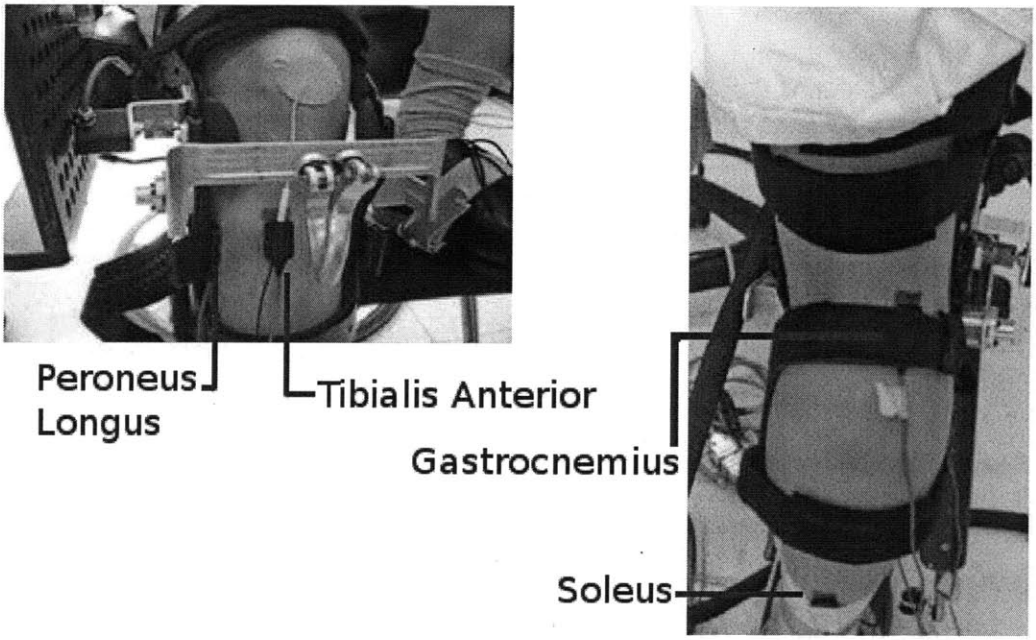

Figure 3-1: Placements of electrodes in impedance measurement experiements. In the left image, bordering the knee brace, the peroneus longus electrode is visible to the left. Immediately to its right, the tibialis anterior electrode is prominent. In the right image, the gastrocnemius electrode is on top, and the soleus electrode is on the bottom.

one muscle with significant amplitude and the rest at low level. In practice, activation of one muscle would often activate nearby muscles (though not antagonists). In the cocontraction condition, subjects were directed to explicitly achieve target muscle amplitudes on several muscles simultaneously. Subjects self-modulated muscle activation based on a visual display of mean EMG. Throughout the course of the study two different visual displays were used. The first display method projected EMG recordings in real time on an oscilloscope, and the target activity level was represented by lines on the display representing the desired EMG amplitude. The second display method displayed the current estimated EMG amplitude to the subject on a computer monitor, represented by the size and position of a horizontal bar on a triangular background (Figure 2.2). The target EMG amplitude represented as the base of the triangle.

In the active experiment subjects were asked to generate a nominally constant unilateral torque. The high activation level of the target muscle relative to the passive condition was

Table 3.1: EMG Activation Amplitude versus Passive Case

Muscle	Tibialis Active (normalized by passive EMG amplitude)	Soleus Active (normalized by passive EMG amplitude)
Tibialis Anterior	9.31	1.13
Peroneus Longus	3.72	2.61
Soleus	1.68	5.58
Gastrocnemius	1.04	1.12

significant and sustained (Table 3.1). However, two limitations to voluntary motor control were observed. First, subjects self-reported difficulty maintaining constant muscle activation when the ankle was perturbed in particular directions. Second, instructing subjects to activate one muscle exclusively proved to be impractical (Table 3.1). In the active condition, some co-activation was observed in every muscle even though instructions were to maintain activity in only one muscle. This may partially explain why there were no significant differences in the shape or magnitude of the impedance function between the two active conditions reported here (Figures 3.2-3.5).

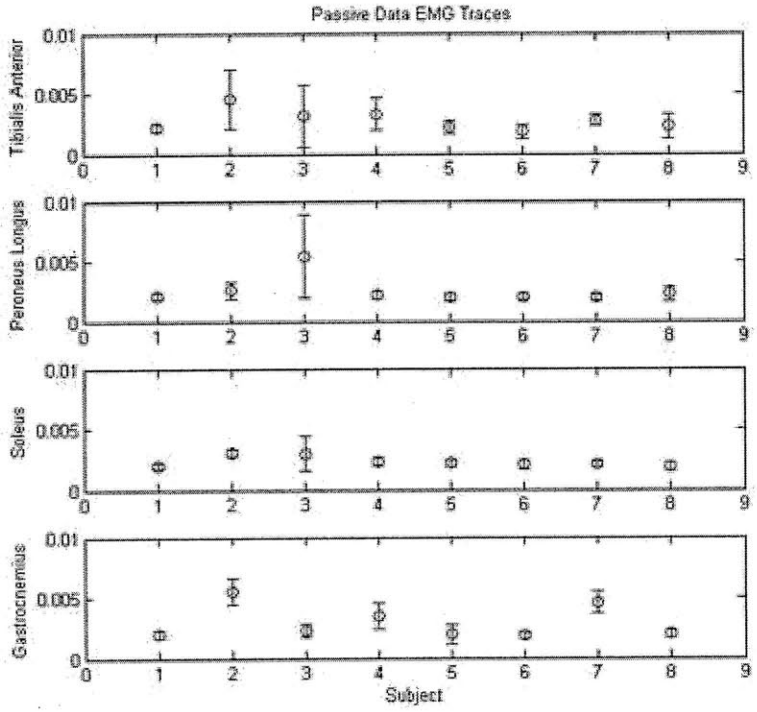

Figure 3-2: Passive EMG Amplitudes (Circle indicates mean, whiskers indicate standard deviation)

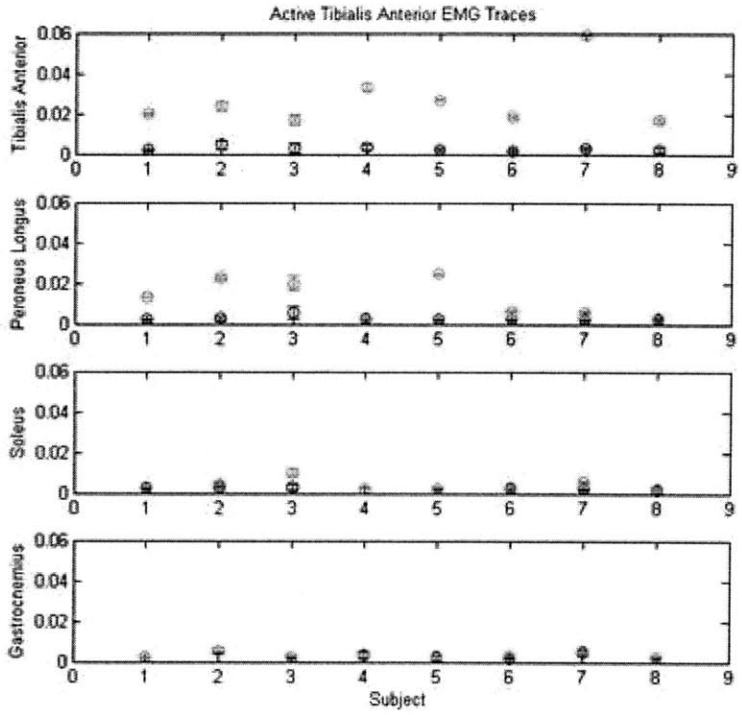

Figure 3-3: Tibialis Active EMG Amplitudes (circle indicates mean, whiskers indicate standard deviation. Blue corresponds to muscles passive and green to muscles active)

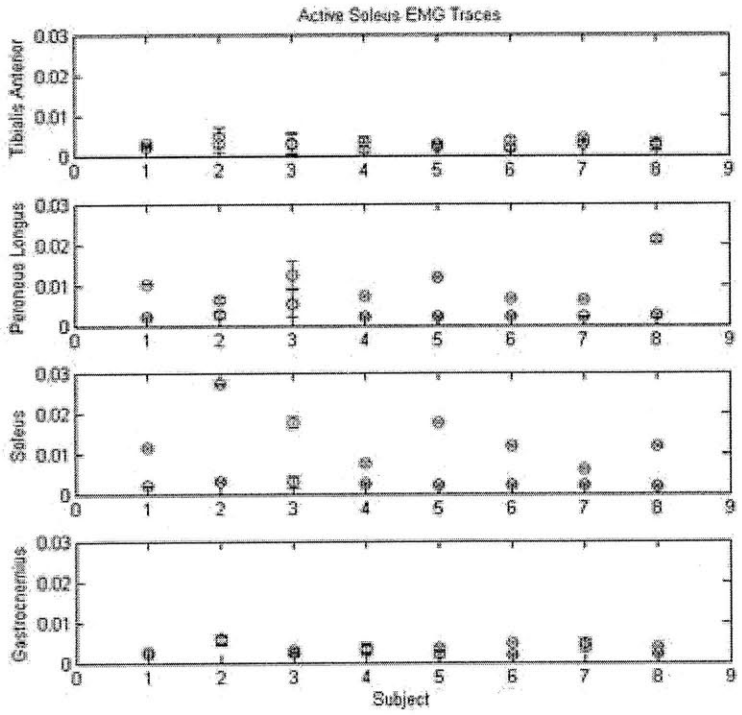

Figure 3-4: Soleus Active EMG Amplitudes (circle indicates mean, whiskers indicate standard deviation. Blue corresponds to muscles passive and red to muscles active)

Chapter 4

Data Analysis and Results

Logged data from the robot consists of the time-histories of torques and angular displacements of the ankle sampled at 200Hz. Each ramp perturbation was logged in a separate file (one inbound ramp and one outbound ramp per move). The static component of impedance for each direction was obtained by computing the slope of a linear least squares fit of the displacement and torque data in that direction (excluding the first 0.5 seconds of each ramp displacement to allow servo-induced transients to dissipate). In three measurements from the passive study, there was a controller error in the final segments of the ramp which was omitted from further analysis. The controller error caused abnormally high torque values to be output through the anklebot if the actual displacement of the foot was small, resulting in inaccurate impedance estimates. This was resolved by estimating impedance with data taken before the onset of the error in a log.

We did not assume an a priori structure to ankle stiffness (aside from the linear approximation in each measured direction), but we have obtained characteristic repeatable shapes for the ankle impedance function. By sampling the impedance function along 24 directions, the two-dimensional shape of ankle impedance emerges. The estimated impedance values of all subjects in the passive study are plotted below. Passive impedance measurements were obtained from 14 subjects (7 female, 7 male). The estimated passive impedance along a direction of perturbation in Figure 4.1 is represented by the magnitude in the radial direction.

Female subjects are indicated by solid lines, and male subjects are indicated by dashed lines. The curves in the figures indicate the impedance of the ankle being perturbed towards or away from the neutral position in a particular orientation. In our numbering scheme, 0 degrees corresponds to a movement of pure eversion, while 90 degrees denotes pure dorsiflexion, and so on. The mean impedance across all subjects varied from a minimum 6.62 N-m/rad at the orientation 195 degrees to a maximum 17.62 N-m/rad at the orientation 90 degrees. The standard deviations varied between 1.83 N-m/rad to 7.35 N-m/rad. The coefficients of variation, defined as standard deviation over mean, varied from .26 to .44.

Of note, not all subjects had symmetrical ankle impedance shapes. In subject KMs case, the impedance in plantarflexion was significantly higher than in dorsiflexion. In subject RHs case, the opposite was true, with impedance in dorsiflexion greater than impedance in plantarflexion. This high subject-to-subject variability means that any statement about a mean impedance shape needs to be qualified with caution about the applicability to a particular case.

Figure 4.2 plots the impedance values of 8 subjects (4 female, 4 male) activating their tibialis anterior muscles. The color scheme is consistent between figure 4.1 and figure 4.2, and in 7 of 8 cases there is a significant increase in ankle impedance. The variation between adjacent directions increases slightly in the tibialis active case, probably due to the fact that muscle activation was not constant from direction to direction. Similar to the passive case, several subjects showed asymmetric impedance shapes (JA, YS, RH). Notably, the impedance function for subject KM increased in symmetry in this case.

Figure 4.3 shows the soleus active condition of seven subjects (4 female, 3 male). The color scheme is consistent with figure 4.1. Ankle impedance is clearly elevated from a passive baseline. This condition showed the highest deviation from a constant amplitude muscle activation from direction to direction. In particular, the perturbation in the the 105 degree direction generally encountered the largest resistance. This could indicate that in this direction of perturbation, the soleus muscle is completely aligned with the action of the robot and therefore contributing a large impedance value. Subject to subject variation remains

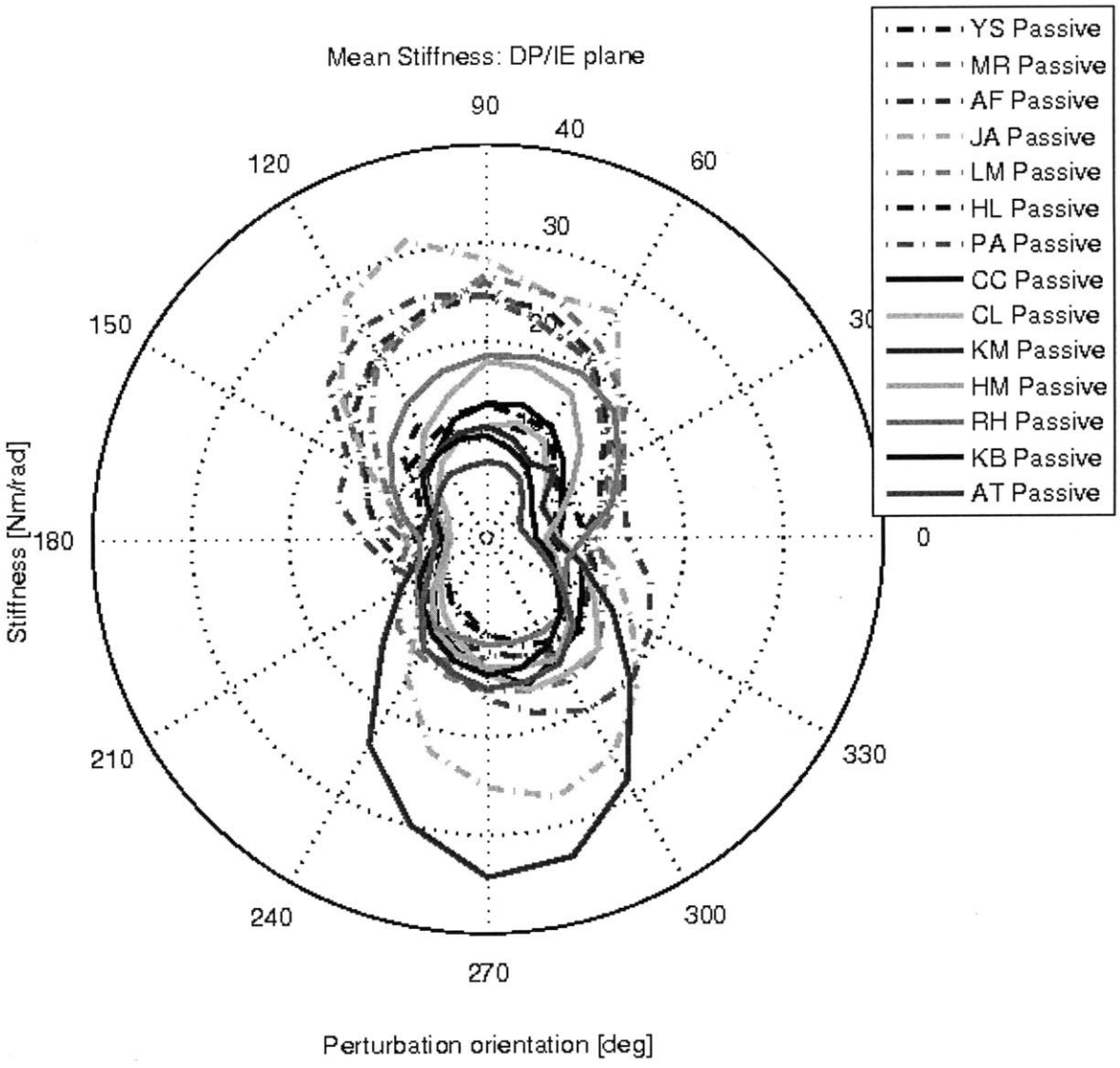

Figure 4-1: Ankle Impedance in Passive Subjects

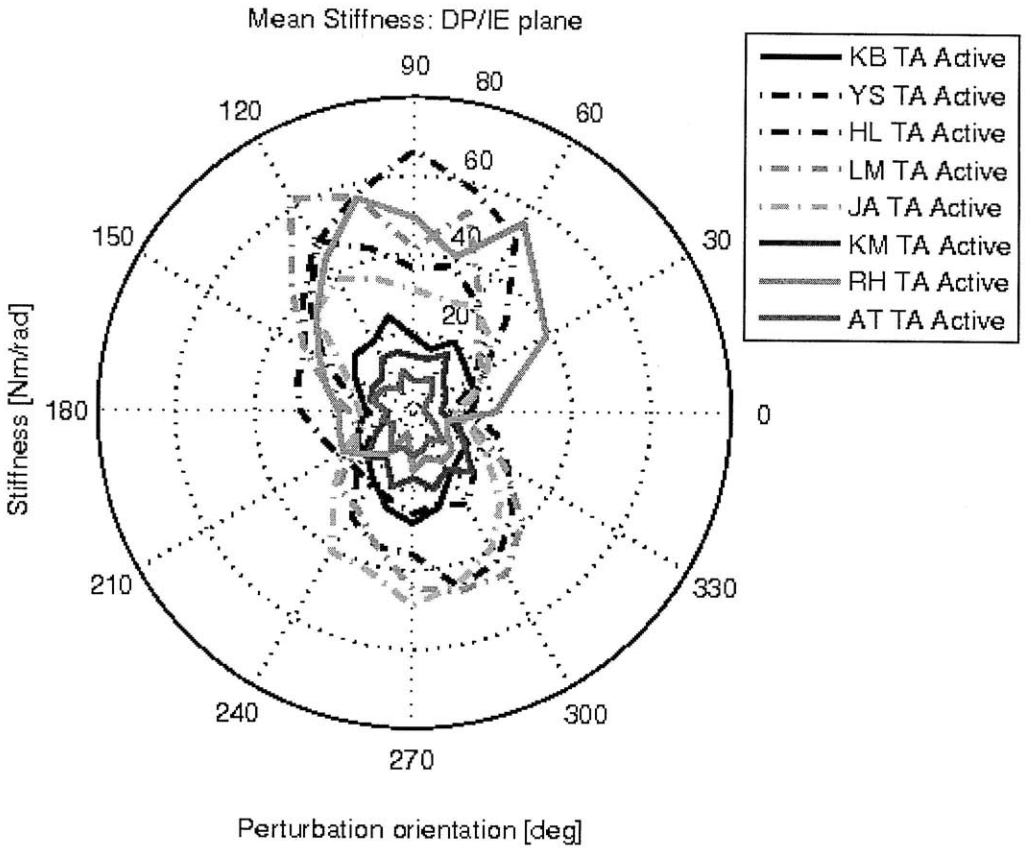

Figure 4-2: Ankle Impedance with Tibialis Anterior Active

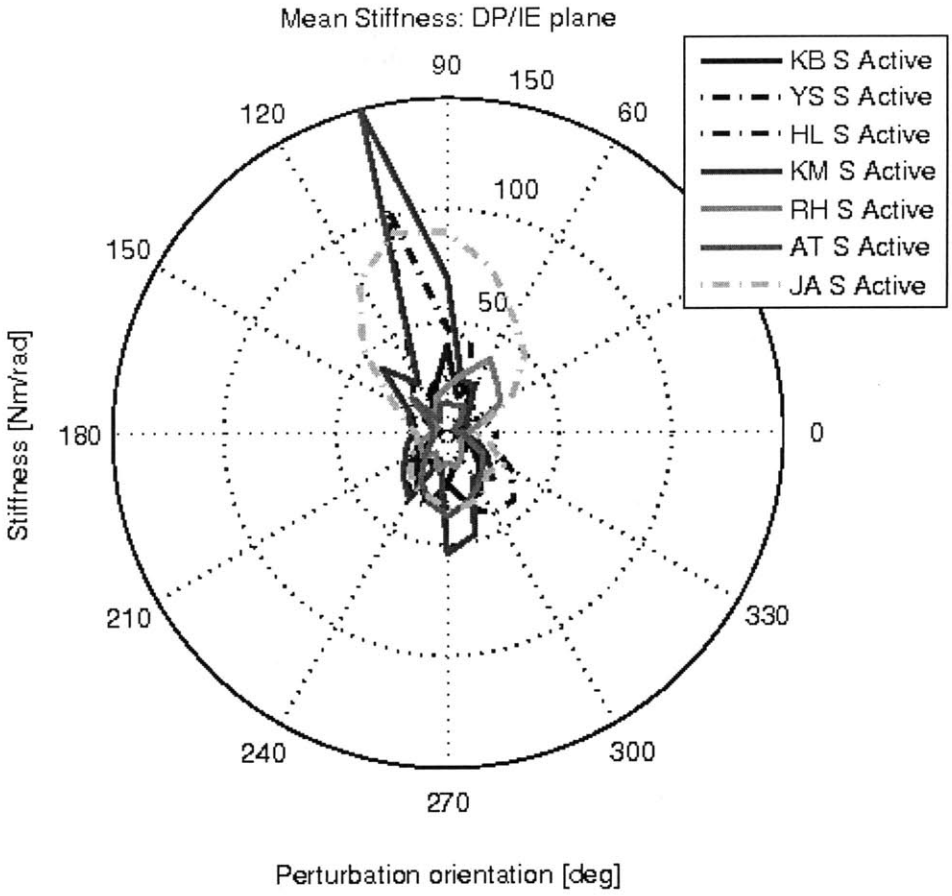

Figure 4-3: Soleus Active Ankle Impedance

high in this case.

Cocontraction impedance measurements were obtained from 8 subjects (3 female, 5 male). The color scheme in Figure 4.4 is consistent with the passive figure (Figure 4.1). Mean impedances ranged from 17.6 N-m/rad at 0 degrees perturbation (pure eversion) to 69.2 N-m/rad at 90 degrees perturbation (dorsiflexion). Standard deviations among all subjects ranged from 6.05 N-m/rad to 30.00 N-m/rad, significantly larger than the passive case. The variation among impedance measured in adjacent directions is greater in cocontraction than in the passive case, indicating that subjects may have had difficulty with maintaining a constant level of muscle cocontraction. However, it is clear that the magnitude of ankle impedance increases despite the large variations from direction to direction.

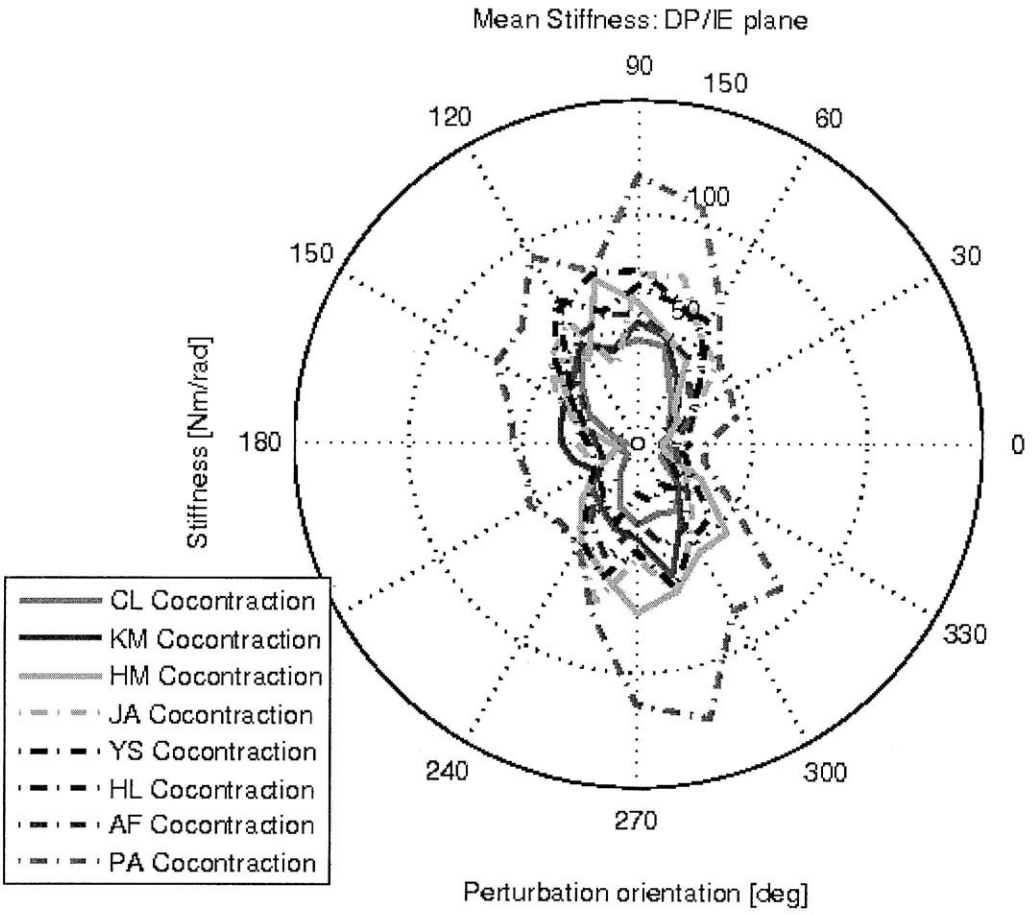

Figure 4-4: Cocontraction Subjects

Table 4.1: Average Measured Static Impedance from All Subjects (N-m/Rad, Mean ± Standard Error)

	Passive N=14	Tibialis Anterior Active N=8	Soleus Active N=7	Cocontraction N=8
Eversion	8.48±0.74	11.24±1.92	11.50±1.94	17.58±2.40
Inversion	6.94±0.68	14.22±2.52	10.53±1.65	23.34±5.39
Dorsiflexion	17.62±1.91	33.27±6.89	38.64±8.40	69.22±7.80
Plantarflexion	15.26±1.79	28.29±4.96	29.86±3.95	52.23±10.2

The mean impedance values in the primary directions are shown in Table 4.1. It is clear that ankle impedance increases in all directions, but more significantly in dorsiflexion and plantarflexion than in inversion and eversion. Cocontraction increases impedance above both active conditions, as well.

Chapter 5

Discussion and Analysis

5.1 Effect of Muscle Activation

The most obvious feature of figure 5.1 is that muscle activation significantly affects the magnitude of ankle impedance. In fact, impedance in any given subjects ankle doubles or triples depending on the experimental condition. Under the conditions of our experiments, co-contraction of antagonist lower leg muscles increased ankle impedance the most. Table 5.1 presents the effect of muscle activation on the measured stiffness (the average factor of increase for all subjects in all directions of motion under that condition). The ability to alter ankle impedance voluntarily is probably important for humans to maintain stable postures and gaits, and our data show that sub-maximal activation of muscles gives humans access to a wide range of impedances. Activating a muscle to generate unilateral torque increases ankle impedance in all directions, even those antagonistic to that muscles action. Table 1 also shows that under one way muscle activation, there is no statistically significant difference in the increase in impedance in IE versus the impedance values in DP. Nonetheless, when muscles are cocontracting, impedance increases much less in the frontal plane than in the sagittal plane (with 95% confidence). This is a clinically important result, as injury commonly occurs from rolling the ankle in the frontal plane [3]. A lower stiffness indicates less resistance to rolling and contraction of the major dorsi- and plantar-flexors does little

Table 5.1: Mean Ratio of Active Impedance versus Passive Impedance in All Directions

	Tibialis Anterior Active	Soleus Active	Cocontraction
Ratio of Increase	1.972±0.061	2.018±0.098	3.238±0.105
F-test Ratio (variation by direction)	0.86	2	3.39
Level needed for significance (95% confidence)	2.95	3.01	2.95

to increase protection against this kind of injury.

5.2 Modeling Ankle Impedance

Another observationequally true, though perhaps less obviousis the unsuitability of stiffness ellipses to represent the static impedance of the ankle, even in the passive condition. Visualizing ankle impedance in both degrees of freedom makes it clear that static ankle impedance is nonlinear: directional variation of measured stiffness departs from the symmetrical shape of any linear representation of impedance. Most strikingly, the shape of the static impedance function is pinched on the inversion-eversion axis. This pinched distribution is still clearly evident when dorsiflexors or plantarflexors are active. On the other hand, it is clear that some structure is present in the ankle impedance function, and that some simple model can be used to describe the 24 impedance estimates measured from each subject.

The ankle impedance shape is a periodic function, but it contains both concave and convex features and evidence of significant asymmetry. We propose the use of a finite Fourier series, Equation (5.1), to capture these features in a reduced-order model.

$F(\theta) = a_0 + a_1 * cos(\theta) + b_1 * sin(\theta) + ... + a_n * cos(n\theta) + b_n * sin(n\theta)$ (Equation 5.1)

A Fourier series can exactly match any continuous periodic function given sufficient terms. It is described as a series of simple oscillatory functions of increasing frequency. Practically, a finite Fourier series can capture a significant amount of the variation of a function assumed to be periodic in a limited number of terms. Figure 5.2 shows the least squares 3rd order Fourier series fit of one subjects impedance measurements. A 3rd order fit means that the highest frequency oscillatory component is 3 times the base frequency.

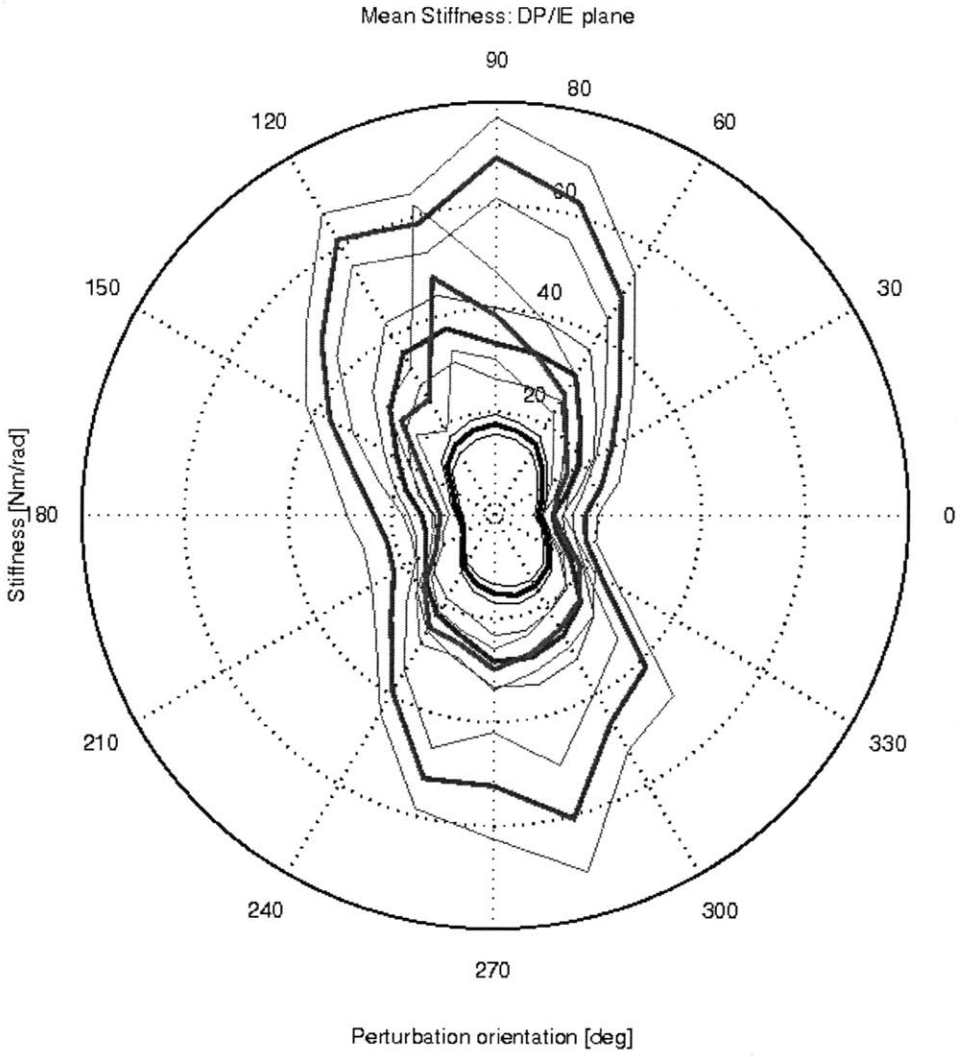

Figure 5-1: Comparison of mean ankle impedances (Mean Measured Passive, Active, and Cocontraction Impedance Values). Thick Line Indicates Mean. Thin Line Indicates 1 Standard Error of the Mean. Solid Black Curve: Passive. Solid Blue Curve: Soleus Active. Solid Red Curve: Tibialis Anterior Active. Solid Green Curve: Cocontraction

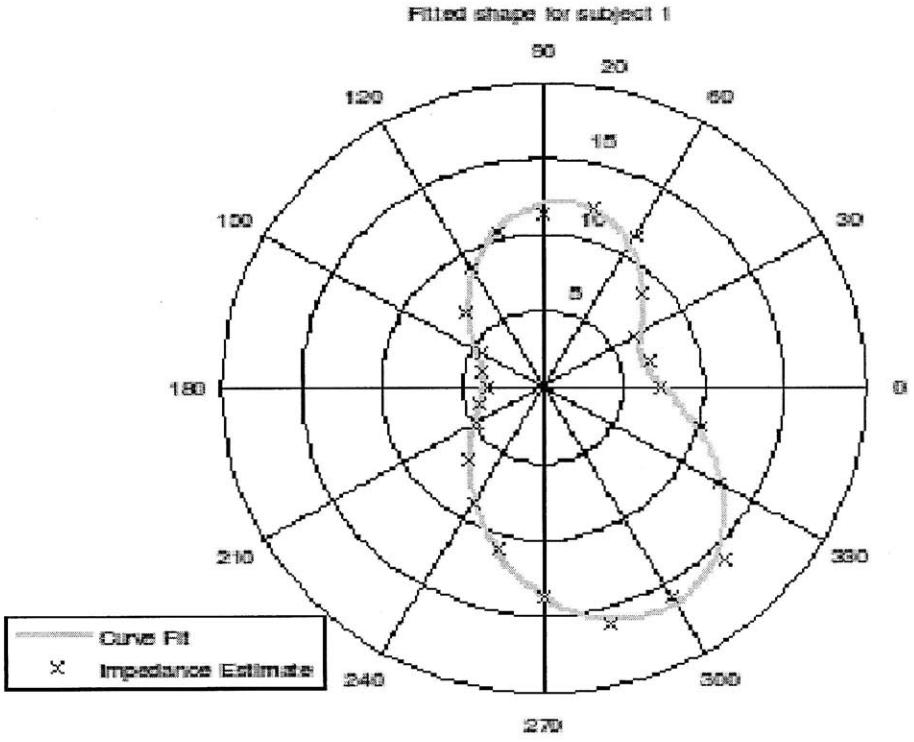

Figure 5-2: Fourier series fit of single subject data

The Fourier series is fundamentally a superposition of several periodic functions. The meaning of each coefficient is a modification of the shape of the final function. Plotted in polar form, the zeroth order term, a_0, creates a circle of radius equal to a_0. Assuming that no higher order terms are larger than the zeroth order term, the area contained within the shape remains constant and equal to the area of the circle with radius a_0. The first order terms eventually shift the function in a single direction, reducing the amplitude in one direction and increasing it in the opposite (as well as distorting the circular shape), with the sine function shifting the function vertically and the cosine function shifting the function horizontally. The net effect is determined by a sum of the sine and cosine terms. The second order sine terms pinches the resulting function along the 45^{o} or 135^{o} line. The second order cosine term pinches the resulting function along the X or Y axes. The third order sine term pinches in three locations, with one pinch locating along the Y axis. The third order cosine term pinches in three locations with one pinch locating along the X axis. The effects of the various Fourier series terms are graphed in figure 5.3.

As shown in figure 5.4, a third-order Fourier series captures at least 80% of the variance of the experimental data measured in this study when its coefficients are determined using least squares fitting. A fourth-order series offers little improvement (if any). A third order model consists of seven parameters, a marked reduction from 24 data points.

By fitting all subjects data to third-order Fourier series approximations, it becomes possible to make comparisons and generalizations about the impedance function shape, independent of the magnitude of ankle impedance. Most importantly, a Fourier series provides a function approximation differentiable along the entire domain of the function. This fact allows reliable estimation of the directions in which ankle impedance is minimal and maximal (by searching for extreme values along the approximation using a numerical method, such as the Newton-Raphson method). Examining the individual impedance functions of all subjects, we find that the local minima and maxima of ankle impedance are not exactly co-aligned with the cardinal directions, though the misalignment is modest (Table 5.2 and Figure 5.5). Ankle impedance was lowest along the inversion-eversion axis, independent of

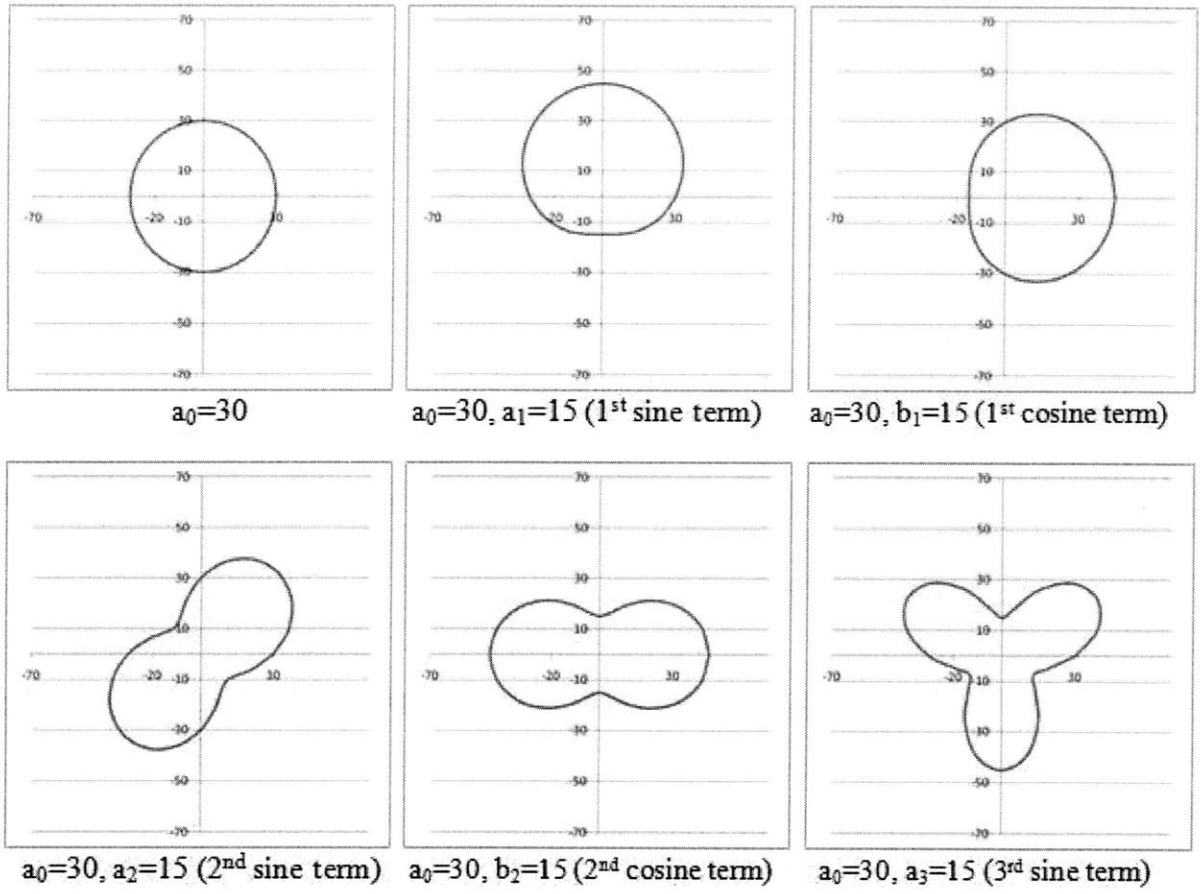

Figure 5-3: Shape contribution of individual Fourier components

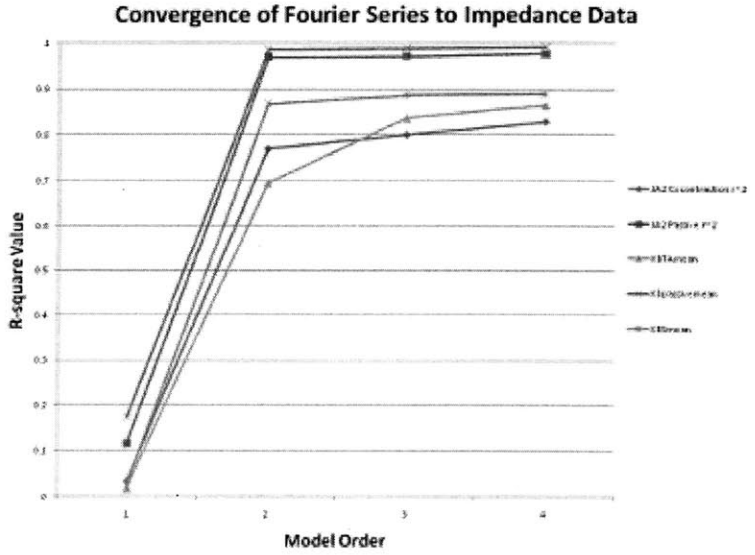

Figure 5-4: Convergence of Fourier Series to Measured Data in Representative Subjects

Table 5.2: Directions of Local Minimum and Maximum Ankle Impedance in Degrees

	Min	Max	Min	Max
Passive	6.1	89.9	191.4	289.1
Cocontraction	0.6	95.4	194.1	273.4
TA Active	-3.4	98.5	163.1	283.7
S Active	5.4	92.7	175.0	251.0

muscle activation.

The average magnitude of a particular subjects impedance is captured in the zeroth-order term of the series (Table 5.3). Normalizing with respect to this term gives the resulting impedance function a constant area. In polar coordinates, even-subscript terms of the Fourier series will produce shapes that are symmetric about two perpendicular axes of symmetry. Odd-subscript terms, however, will produce shapes symmetric about an odd number of nonperpendicular axes. The magnitude of the odd-subscript terms can thus be used as a measure of the distortion or asymmetry of a subjects ankle impedance function.

Figure 5.6 shows the magnitude of the Fourier coefficients derived from both studies. The terms at each successive order are normalized by the zeroth-order term. Note that most subjects exhibit significant first-order terms, indicating a significant deviation of their ankle impedance away from symmetry about two axes. It is also important to note that among these healthy young adult subjects, there is significant variation of ankle impedance shape. Some of this variability may be attributed to experimental variability in the procedure. However, the repeatable nature of these measurements indicate that variation among individuals is large and the average impedance shape obtained in a study is expected to be highly sample dependent. With muscles relaxed (passive) many subjects show small-to-moderate odd

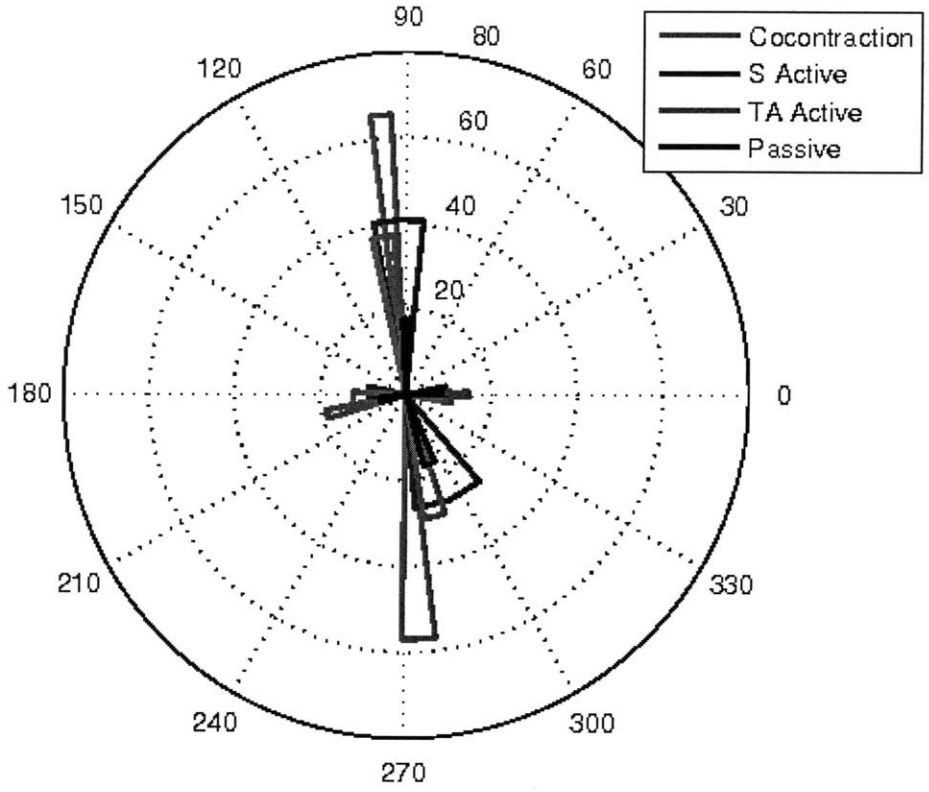

Figure 5-5: Maximum and Minimum Impedance Values

Table 5.3: Average Ankle Impedance by Subject and Activation Condition (N-m/rad)

Subject	Gender	Passive a_0	TA Active a_0	S Active a_0	Cocontraction a_0
YS	M	10.84	26.27	14.58	41.26
HL	M	12.84	32.27	29.2	34.28
JA	M	12.6	27.84	34.48	42.08
LM	M	15.7	32.19		
AF	M	14.25			33.44
PA	M	17.18			69.00
KM	F	15.23	13.37	27.97	32.37
RH	F	12.23	26.09	13.56	
KB	F	8.677	18.16	18.71	
AT	F	8.234	7.755	16.01	
CL	F	9.246			23.58
HM	F	10.41			38.27

coefficients, but under different muscle activity those same subjects exhibit relatively large odd coefficients. This may be due to muscle tone, exercise habits, previous injury, or other factors, though as yet we have not pursued this line of investigation.

As the odd Fourier coefficients represent asymmetry or skew of the impedance function, what might the even coefficients represent? Equations 5.2 through 5.4 show that the second-order terms are consistent with a simple linear model of ankle impedance. Assume that ankle impedance is determined by two independent linear stiffnesses, K_{DP} and K_{IE}. K_{DP} exerts a conservative force along the DP axis, proportional to sin(θ) (Equation 5.2). K_{IE} exerts a conservative force along the IE axis, proportional to cos(θ) (Equation 5.3). Using our method of measuring and representing ankle impedance, the measured impedance is back-projected along the direction of displacement, thus yielding $sin^2(\theta)$ along the DP axis and $cos^2(\theta)$ along the IE axis (Equation 5.4a). With a little algebra this can be shown to be equivalent to a constant (zeroth-order) term plus a second-order cosine term (Equation 5.4b). Thus the zeroth-and second-order terms represent those components of ankle static mechanical impedance that can be attributed to a linear spring-like behavior.

$T_{DP}(x,\theta) = K_{DP} * x_n * sin(\theta)$ Equation 5.2, Stiffness in DP Direction due to equivalent single spring

$T_{IE}(x,\theta) = K_{IE} * x_n * cos(\theta)$ Equation 5.3, Stiffness in IE direction due to equivalent

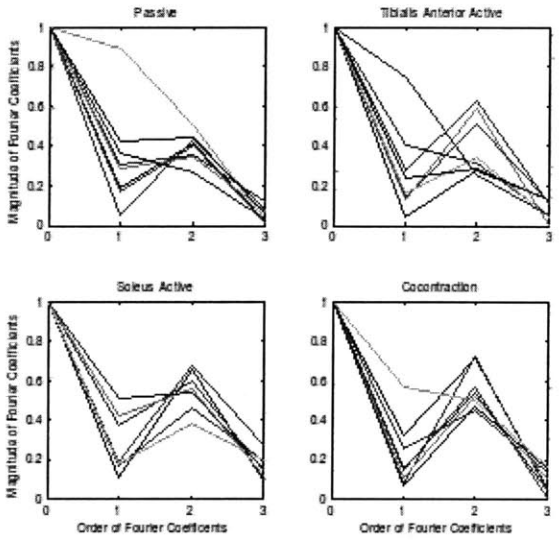

Figure 5-6: Fourier Coefficients from Experimental Fits, Displaying Shape Properties of Ankle Impedance.

single spring

$F_{proj}(\theta) = K_{DP} * sin^2(\theta) + K_{IE} * cos^2(\theta)$ Equation 5.4, Torque projected parallel to line of perturbation

$F_{proj}(\theta) = K_{DP}/2 * (1 - cos^2(\theta)) + K_{IE}/2 * (1 + cos(2\theta))$

$F_{proj}(\theta) = (K_{DP}/2 + K_{IE}/2) + (K_{IE}/2 - K_{DP}/2) * cos(2\theta)$ Equation 5.4b, zeroth and second order cosine components of two-spring model.

Much of the observed variance is consistent with a linear two-spring model. However, the presence of asymmetry in all muscle conditions indicate that some natural variance in human ankle impedance cannot be captured by a linear two-spring model. Using a Fourier series representation provides a compact, intuitive, and convenient method for recording ankle impedance data, enabling further quantitative study of the biomechanics of the ankle beyond a simple spring-based model.

Chapter 6

Conclusion

Humans modulate ankle stiffness in the course of using their leg muscles. If a therapeutic robot is to properly assess ankle impedance, accounting for muscle activation is necessary. Using Anklebot we have shown that, the effect of muscle stiffness modulation can be measured in vivo with much greater detail and precision than has been reported previously. A reliable method of characterizing active impedance may prove important for future developments in haptics, medical robotics, and physical therapy. The study reported here has revealed that ankle static impedance has a surprisingly rich structure. Further work is needed to characterize the biomechanical origin of the directional distribution of stiffness. These and other Anklebot-enabled studies promise to increase our knowledge about the dynamic structure of ankle impedance, improving human-robot interaction and therapy.

6.1 Recommendations for Future Work

This study developed a quantitative and interpretive description of human ankle impedance, as well as a method for collecting data suitable for generating that description. Future work remains in collecting impedance measurements from a wider range of ages and health conditions to determine the normal biomechanical properties of the human ankle (as well as to improve our understanding of whether there are signature traces in human ankle impedance

based on health or biomechanical differences). There is also the potential to explore automation of the collection of ankle impedance data. A computer program which quickly generates Fourier series after an impedance measurement could provide a fast and powerful diagnostic tool, allowing clinicians to immediately determine a subjects ankle impedance and not rely on lengthy data processing procedures. Refinement to the model of ankle activity as passive, active, or cocontracting could be done. A quantitative model relating muscle activity to ankle impedance remains to be found- in this study we did not examine the effect of different levels of activation within the same condition. A future study could examine, for example, the effect of different levels of cocontraction on impedance. Lastly, work on dynamic forms of ankle impedance will also deepen our understanding of human ankle impedance.

Appendix A

Using Anklebot Software to Measure Ankle Impedance

A.1 Preparation for experiment

1.Ensure that anklebot, the computer, and the EMG system are all turned on and functional. 2.Clean off the EMG Electrodes 3.Have the subject wear the anklebot shoes 4.Place the knee brace on the subject 5.Attach reference electrode to subject 6.Attach measurement electrodes to subject 7.Connect anklebot to the subject

A.2 Run CocontractionStudy.tcl

2-1 Type wish CocontractionStudy.tcl to begin the program 2-1.1 On the old system, use su to change the root user. On the new system, this step is not necessary.

2-2 Center the subjects foot in the initial position using a goniometer.

2-3 Respond to the prompt with y in order to record the initial foot position and zero the linear encoders at the initial foot location. If this is not desired respond with n.

2-4 Enter a descriptive name for the trial. All data logged by this program will be saved in the folder: /home/imt/anforce/DATE/TRIALNAME where DATE is the day the

measurement was taken and TRIALNAME is the name the user inputs 2-5 Press enter again to begin the controller software. Once the controller software is running the actuators should be stiff to the touch and resist perturbations away from the encoders zeroed position. 2-6 The EMG amplitude estimation is now ready to run. The program will ask if the user wishes to remove the DC bias in all the DAQ channels. Enter y if the DC bias of the amplitude estimation needs to be removed. Enter n if the old bias measurements are not to be cleared.

2-7 The standard perturbation profile we use is a ramp input of 20 degrees amplitude with velocity 5 degrees per second, with .1 second pauses between ramps. 2-8 Once the perturbation profile is entered into the program, the experimenter should open a new terminal and run the display program.

A.3 Run wedgedisp.tcl

3-1 Open a new terminal and move to the folder where wedgedisp.tcl is saved 3-1.1 Change to root user if necessary 3-2 Begin the visual display by typing in wish wedgedisp.tcl

3-3 If the robot is operating as it should, the screen will appear the following way.

3-4 Begin the amplitude estimation display by pressing run

3-5 If needed, rescale the display wedges 3-5.1 Each display wedge is assigned a displayref variable. To rescale the display wedge, determine a new reference value by entering displayrefX 1 into the pink box and clicking write shm (where X is the index of the wedge).

displayref0 Default variable: ampest0

displayref1 Default variable: ampest1

displayref2 Default variable: ankle_dp_torque

displayref3 Default variable: ampest2

displayref4 Default variable: ampest3

displayref5 Default variable: ankle_ie_torque

3-5.2 Writing shm with a displayref command will cause the terminal to output the instantaneous value of that display wedge. Use this value to determine a new reference value. 3-5.3 To rescale, quit out of the wedgedisp.tcl program 3-5.4 Enter the command

emacs wedgedisp.tcl 3-5.5 Change the value following the commands, set arr(X,ref) , on lines 55-65, where X is the index of the wedge 3-5.6 Save changes 3-5.7 Restart wedgedisplay.tcl by typing in wish wedgedisplay.tcl into the command prompt. 3-6 Once the program is active the subject can monitor their muscle activity state visually, and follow the experimental condition 3-7 Return to the first terminal (CocontractionStudy.tcl) and enter y to begin moves.

3-8 The program will move through the 24 directions protocol and save the data to a log folder determine by name 3-9 Convert the data to ascii by going to the log folder. Use the command source FILEPATH/converter FILEPATH is the location of the document converter

Bibliography

[1] H Gomi and R Osu. Task-dependent viscoelasticity of human multijoint arm and its spatial characteristics for interaction with environments. *Journal of Neuroscience*, 18:8965–8978, September 1998.

[2] FA Mussa-Ivaldi, N Hogan, and E Bizzi. Neural, mechanical and geometric factors subserving arm posture in humans. *Journal of Neuroscience*, 5:2732–2743, 1985.

[3] D.H O'Donoghue. *Treatment of injuries to athletes.* Saunders Company, 1984.

[4] A Roy, HI Krebs, DJ Williams, CT Bever, LW Forrester, RM Macko, and N Hogan. Robot-aided neurorehabilitation: A novel robot for ankle rehabilitation. *IEEE Transactions on Robotics*, 25(3):569–582, 2009.

[5] RW Selles, XY Li, F Lin, SG Chung, EJ Roth, and LQ Zhang. Feedback-controlled and programmed stretching of the ankle plantarflexors and dorsiflexors in stroke: Effects of a 4-week intervention program. *Arch Phys Med Rehabil*, 86(3):2330–2336, December 2005.

[6] RW Selles, CY Yeh, JJ Chen, and KH Tsai. Quantitative analysis of ankle hypertonia after prolonged stretch in subjects with stroke. *Journal of Neuroscience Methods*, 137:305314, 2004.

[7] T Sinkjaer, E Toft, S Andreassen, and BC Hornemann. Muscle stiffness in human ankle dorsiflexors: Intrinsic and reflex components. *Journal of Neurophysiology*, 60(3):1110–1121, September 1988.

[8] FE Zajac. Muscle and tendon: properties, models, scaling, and application to biomechanics and motor control. *Crit Rev Biomed Eng*, 17(4):359–411, 1989.

[9] SM Zinder, KP Granata, DA Padua, and BM Gansneder. Validity and reliability of a new in vivo ankle stiffness measurement device. *Journal of Biomechanics*, 40:463–467, 2007.